# *N*-Sulfonyl homoserine lactones as antagonists of bacterial quorum sensing

Sandra Castang,[a] Bernard Chantegrel,[b] Christian Deshayes,[b] René Dolmazon,[b] Patrice Gouet,[c] Richard Haser,[c] Sylvie Reverchon,[a] William Nasser,[a] Nicole Hugouvieux-Cotte-Pattat[a] and Alain Doutheau[b,*]

[a]*Unité de Microbiologie et Génétique, UMR CNRS-INSA-UCB 5122, Bât. A. Lwoff, UCB, 69622 Villeurbanne, France*
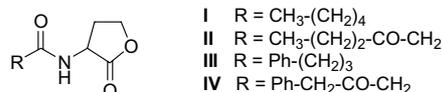[b]*Laboratoire de Chimie Organique, UMR CNRS-UCB-CPE 5181, Bât. J. Verne, INSA, 69621 Villeurbanne, France*
[c]*Laboratoire de Bio-Cristallographie, Institut de Biochimie et Chimie des Protéines, UMR CNRS-UCB 5086, 7 Passage du Vercors, 69367 Lyon Cedex 07, France*

**Abstract**—A series of 11 new analogues of *N*-acylhomoserine lactones in which the carboxamide bond was replaced by a sulfonamide one, has been synthesised. These compounds were evaluated for their ability to competitively inhibit the action of 3-oxohexanoyl-L-homoserine lactone, the natural ligand of the quorum sensing transcriptional regulator LuxR, which in turn activates expression of bioluminescence in the model bacterium *Vibrio fischeri*. Several compounds were found to display antagonist activity. Molecular modeling suggests that the latter prevent a cascade of structural rearrangements necessary for the formation of the active LuxR dimer.

Diverse bacteria regulate the expression of specific gene systems through the exchange of diffusible extracellular signaling molecules called autoinducers.[1] A link between this process, termed quorum sensing (QS), and virulence[2] or the formation of biofilms[3] has been established for a number of pathogenic bacteria suggesting that interference with these signaling circuits might be therapeutically useful. For many Gram-negative bacteria the autoinducers are members of a family of compounds known as *N*-acyl-L-homoserine lactones (AHSLs) which differ in the length and substitutions of their acyl chain. For instance, the marine luminescent bacterium *Vibrio fischeri* produces AHSLs **I** and **II** (Scheme 1) as main autoinducers.[4,5] These autoinducers bind to their cognate transcriptional regulatory proteins (LuxR in the case of *V. fischeri*) and induce their dimerisation. The QS regulators are composed of a ligand receiver domain, which binds AHSL and of a regulator domain, which interacts with DNA. The active dimer complex interacts with specific DNA sequence and promote transcription of genes containing this target motif in their promoter



| | |
|---|---|
| **I** | R = CH₃-(CH₂)₄ |
| **II** | R = CH₃-(CH₂)₂-CO-CH₂ |
| **III** | R = Ph-(CH₂)₃ |
| **IV** | R = Ph-CH₂-CO-CH₂ |

**Scheme 1.** Structures of autoinducers **I**, **II** and antagonists **III**, **IV**.

region (the *lux*CDABEG operon for *V. fischeri*). Recent crystal structure of a QS transcriptional regulator, TraR from *Agrobacterium tumefaciens*, bound to its autoinducer, showed that the particular aminoacids residues with which AHSLs establish specific contacts are highly conserved among all the QS regulators.[6,7]
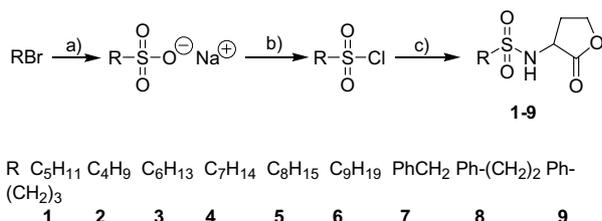
Considering the therapeutic possible applications, an important effort has been devoted to the design of potential antagonists of QS, particularly AHSLs analogues.[8] The described AHSLs analogues mainly belong to two families: compounds modified by replacement of the γ-butyrolactone ring by other heterocycles or carbocycles and compounds differing from the natural inducers by the nature of the acyl chain. Most members of the first class proved to be inactive excepted analogues bearing either a cyclopentanol[9] or a phenol[10] in place of the lactone. Compounds belonging to the second class were

* Corresponding author. Tel.: +33 472 43 82 21; fax: +33 472 43 88 96; e-mail: alain.doutheau@insa-lyon.fr
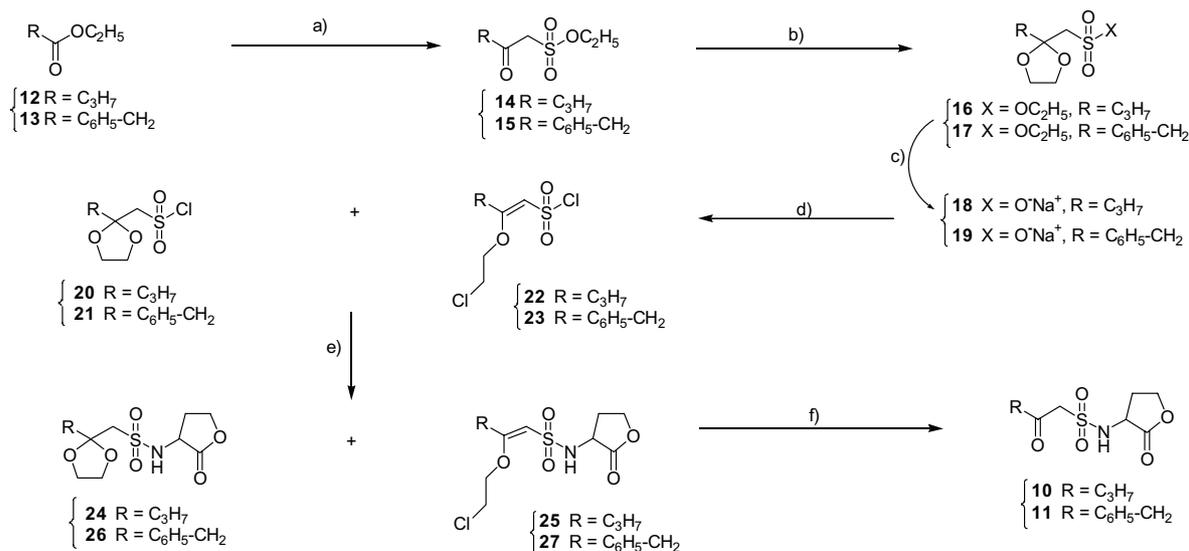
found to be either agonists or antagonists depending on their structural features.[1] We recently reported[11] that analogues bearing an aromatic ring at the extremity of the alkyl side chain displayed antagonist activity, the most active of them being the compounds **III** and **IV** (Scheme 1). In our pursuit of identifying new inhibitors of quorum sensing, we have now prepared and tested in the *V. fischeri* model, a series of new AHSLs analogues in which the carboxamide function has been replaced by a sulfonamide one. Although sulfonamides show widespread biological activity, only recently[12] has the activity of these types of compounds on quorum sensing been examined.

Racemic mixtures of *n*-alkylsulfonyl-HSLs **1–6**, phenylalkylsulfonyl-HSLs **7–9** and 2-oxoalkylsulfonyl-HSLs **10–11** were prepared according to the synthetic sequences depicted in Schemes 2 and 3.[13]

Compounds **1–11** were evaluated for their ability to interfere with the induction of luminescence by *N*-3-oxohexanoyl-L-homoserine lactone (3-oxo-C6-HSL, **II**) in

the *V. fischeri* QS system. We used the recombinant *Escherichia coli* strain NM522 containing the plasmid pSB401 to measure the induction of luminescence by various AHSLs analogues. In pSB401, the *luxR* and the *luxI* promoter from *V. fischeri* have been coupled to the entire *lux* structural operon (*lux*CDABE) from *Photorhabdus luminescens*.[14] The influence of AHSLs analogues on the induction of bioluminescence by 3-oxo-C6-HSL was determined as described previously,[11] except that this inducer was used at a final concentration of 50 nM. This concentration was required for 1/2 maximal induction of luminescence under our conditions. The experiments were done in triplicate and the standard deviation (data not shown) did not exceed 10% of the mean value.

We first tested the *N*-alkylsulfonamides **1** and **10** and the *N*-alkylsulfonamides **9** and **11** structurally related, respectively, to the autoinducers **I** and **II** and to the inhibitors **III** and **IV**. As shown in Figure 1, the replacement of the carboxamide function in autoinducer **I** by the sulfonamide one in compound **1** resulted in a good antagonist activity. By contrast the analogue **10** of autoinducer **II** proved to be inactive. Similarly, the analogue **9** displayed a significant inhibitory activity while the analogue **11** was inactive. Thus, the presence of a sulfonamide function in alkyl substituted derivatives resulted in a pronounced antagonist activity while the combination of 3-oxo and sulfonamide functionalities gave no inhibitory effect.

To evaluate the influence of the alkyl chain length on the activity we next tested the alkylsulfonyl-HSLs **1–6**. As shown in Figure 2, the antagonist activity is clearly affected by the number of carbon atoms in the alkyl chain. The shortest analogue **2** with a butyl chain was poorly active. The maximum activity was found for compound
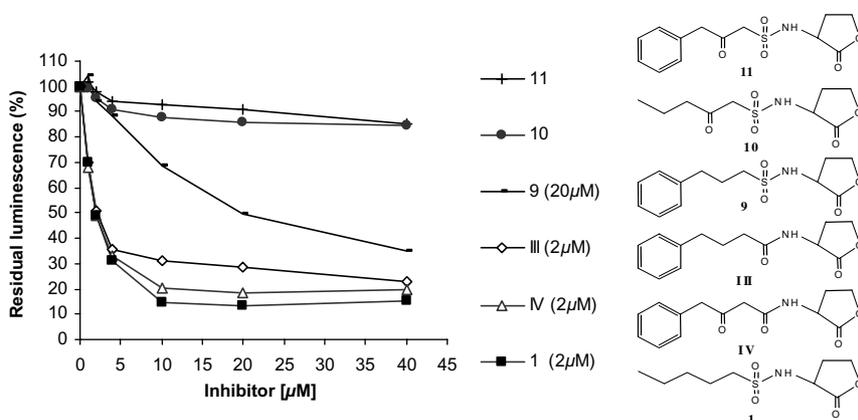
R  $C_5H_{11}$  $C_4H_9$  $C_6H_{13}$  $C_7H_{14}$  $C_8H_{15}$  $C_9H_{19}$  PhCH$_2$  Ph-(CH$_2$)$_2$  Ph-(CH$_2$)$_3$
   **1**       **2**     **3**      **4**      **5**      **6**     **7**      **8**          **9**

**Scheme 2.** Synthesis of sulfonyl-HSL **1–9**. Reagents and conditions: (a) sodium sulfite, water, 24 h reflux; (b) thionyl chloride, benzene, 4 h reflux; (c) α-amino-γ-butyrolactone hydrobromide, 1,8-diazabicyclo[5.4.0]-undec-7-ene, 4-dimethyl amino-pyridine, dichloromethane, 24 h at rt. Yields for step (c) 70–80% for **1–6**, **9** and 50% for **7**, **8**.

**Scheme 3.** Synthesis of sulfonyl-HSL **10**, **11**. Reagents and conditions: LiCH$_2$SO$_3$C$_2$H$_5$, tetrahydrofuran, 1.5 h at −60 °C, then 2 h at rt [yield ∼85%]; (b) ethylene glycol, *p*-toluenesulfonic acid, benzene, 24 h reflux, [yield ∼90%]; (c) sodium iodide, acetone, 24 h rt [yield ∼85%]; (d) triphenylphosphine, sulfuryl chloride, dichloromethane, 16 h at rt [yield ∼35%]; (e) α-amino-γ-butyrolactone hydrobromide, 1,8-diazabicyclo[5.4.0]-undec-7-ene, 4-dimethyl aminopyridine, dichloromethane, 24 h rt [yield ∼55%]; (f) aqueous 95% trifluoroacetic acid, 2 h at rt [yield ∼95%].

**Figure 1.** Antagonist effects of *N*-sulfonyl-HSLs **1**, **9**, **10** and **11** compared to **III** and **IV**. The concentrations (μM) required for 50% inhibition are given in parentheses.
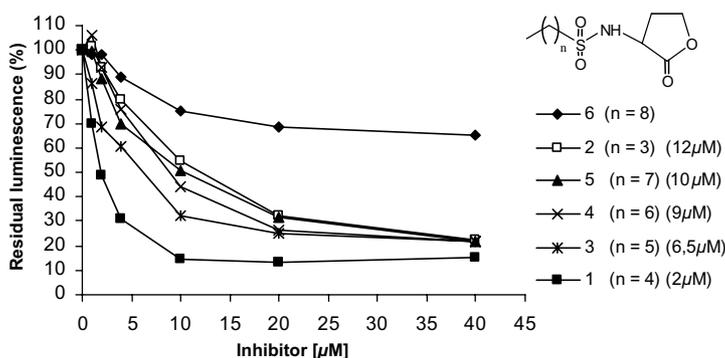


**Figure 2.** Effect of the alkyl chain length on antagonist activity of *N*-sulfonyl-HSLs **1**–**6**. The concentrations (μM) required for 50% inhibition are given in parentheses.

**1** with a pentyl chain. Increasing the chain length from five to nine carbon atoms (compounds **1**, **3**, **4**, **5** and **6**) resulted in a correlated decrease of antagonist activity.

Since compound **9** proved to be partially inhibitor we further examined the influence of the distance between the sulfonamide and the phenyl groups on activity. As shown in Figure 3, when the two groups are spaced by one carbon atom (compound **7**), no significant inhibitory activity could be detected. By contrast, compound

**8** in which these two groups are spaced by two carbons is more active than **9** and almost as active as **1**. Thus, despite no synergy was observed between the sulfonamide function and the phenyl group, the position of the phenyl group appeared important for activity.

In order to get a qualitative understanding of the protein-analogue molecular recognition we first attempted to build a 3D model for LuxR using as template the crystallographic structure of TraR, the only known representative of the LuxR family at present (PDB entries
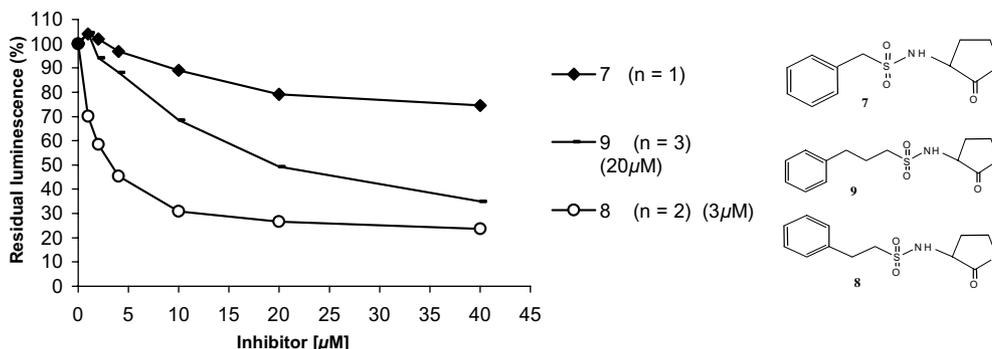


**Figure 3.** Effect of the phenyl group position on antagonist activity. The concentrations (μM) required for 50% inhibition are given in parentheses.
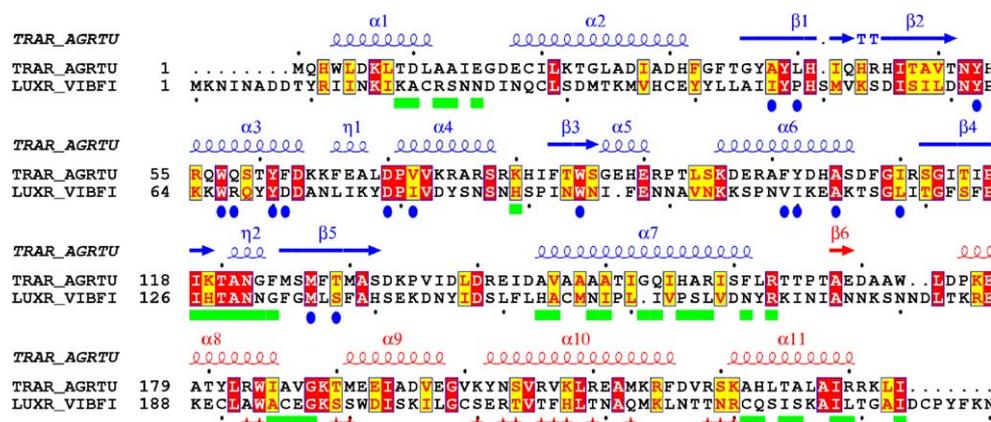
**Figure 4.** Sequence alignment produced by T-COFFEE[17] and drawn with ESPript.[20] Identities are boxed in red. Similarities are boxed in yellow according to physico-chemical properties. Secondary structure elements have been calculated from the 3D structure of TraR (pdb code 1L3L) using the program DSSP.[21] They are displayed on the top of sequence blocks. Alpha and $3_{10}$ helices are represented by squiggles labelled α and η, respectively. Strands are represented by arrows. Secondary structure elements are coloured in blue for the receiver domain and in red for the regulator domain. Residues interacting with the bound AHSL in TraR are marked with blue solid circles, residues interacting with the DNA fragment are marked with red stars, residues in contact at the dimer interface are marked with green squares. Maximum interaction distance is 4 Å.

1H0M and 1L3L determined to 3 Å and to 1.7 Å resolution, respectively).[6,7] Sequences of LuxR and TraR were aligned using various programs: MULTALIN, CLUSTAL and T-COFFEE.[15–17] Scores of identity are low, about 20%, and positions of insertions and deletions vary between programs. Consequently, a complete model for LuxR could not be generated using dedicated servers such as GENO3D or SWISS-Model.[18,19] However, gaps between the two sequences are few in number and short in length (Fig. 4). The three computed alignments are identical for residues located between: (i) the start of strand β2 and the end of strand β3, (ii) the start of helix α6 and the end of strand β5 and (iii) the start of helix α8 and the end of the sequence. Most residues interacting with the AHSL molecule and the DNA fragment in TraR are conserved in LuxR. Thus, the overall fold of TraR must be preserved in LuxR.

We then built a simple model of LuxR from the high resolution structure 1L3L of TraR by using the alignment shown Figure 4 and the program CALPHA[22]: the side chains of the 16 residues of the AHSL binding site were replaced and resting non-glycine residues were substituted by alanines. The resulting model, shown in Figure 5, was analysed on a Silicon Graphics workstation using the SYBYL 6.7 software package.[23] Preferential conformations of synthetic ligands **1**, **8–10** were generated by molecular modeling using the Tripos force-field implemented in the SYBYL program. They were superimposed in turn to the bound AHSL molecule (*N*-3-oxooctanoyl-L-homoserine lactone) contained in 1L3L. Then, every ligand in the closest conformation was manually docked into the active site of LuxR to analyse intermolecular interactions.

This molecular modeling shows that the strongest antagonists **1** and **8** best fit the active site: extremity of their alkyl chain is firmly packed at the entrance of the pocket while their lactone group is tightly bound in the core of the receiver domain. By contrast, sulfonamides **9** and **10** are not well adapted to the protein cavity: in these cases,
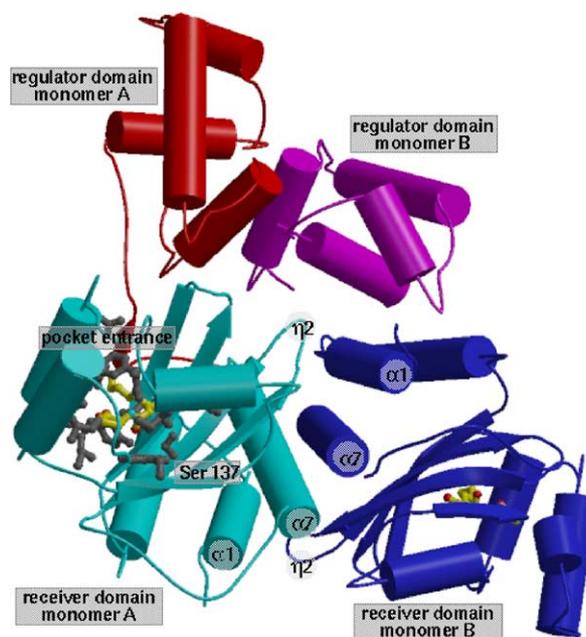


**Figure 5.** Ribbon representation of the dimeric model of LuxR in complex with a homoserine lactone molecule (*N*-3-oxooctanoyl-L-homoserine lactone) as observed in TraR. Alpha helices are drawn as rods and beta strands are drawn as arrows. The bound HSL is represented as ball-and-sticks and coloured by atom type. Modeled residues of the active site are in grey. Secondary structure elements involved in the interface between regulator domains are pointed out. Figure was created with BOBSCRIPT.[24]

modification in the spatial orientation of the alkyl chain due to the change of geometry from trigonal in carboxamide to tetragonal in sulfonamide, no longer permits either the phenyl group in **9** or the keto function in **10** to be correctly positioned in the pocket.

Molecular modeling suggests that the two families of synthetic AHSLs analogues displaying antagonist activity, the carboxamides such as **III** and **IV**[11] and the sul-
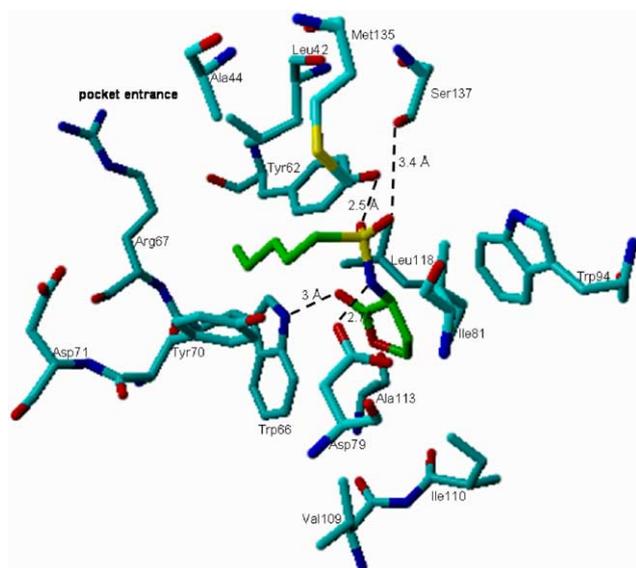
**Figure 6.** Interaction of *N*-pentansulfonyl-L-homoserine lactone (green) with the active site model of LuxR. The figure was drawn with YASARA.[27]

fonamides such as **1** and **8**, may induce two distinct paths of structural rearrangements, which are likely to affect the dimerisation process. On the one hand, the alkyl chain of the autoinducers **I** and **II** is fixed near the interface separating the regulator and receiver domains in a monomer (10 Å) and it can be supposed that analogues **III** and **IV** bearing a phenyl group at the extremity of their alkyl chain are antagonists by perturbing this interface and the dimerisation process. On the other hand, the carbonyl of the carboxamide moiety of autoinducers **I** and **II** points toward the interface separating the receiver domains in the dimer and could be involved in its formation. Distance to this interface, composed of helices α1, α7 and η2 (Figs. 4 and 5), is long (20 Å) but a cascade of structural rearrangements can be proposed. Such long distance mechanism is observed in the dimerisation process of the receiver domain of FixJ, a transcriptional activator protein of a related family.[25] Of particular interest, as shown in Figure 6, a carboxamide to sulfonamide substitution involves new intermolecular contacts with Tyr62 and Ser137 in the core of the receiver domain (Fig. 6) and it has been reported that mutations on the residue equivalent to this serine in TraR, a threonine, alter protein activation.[26]

To conclude, a nonactive protein would be obtained in the two cases, phenyl group at the end of the alkyl chain in carboxamide analogues or sulfonamide moiety in sulfonamides analogues, explaining the observed absence of synergic effect in compounds bearing the two structural modifications.

### References and notes

1. For a recent review, see Lyon, G. J.; Muir, T. W. *Chem. Biol.* **2003**, *10*, 1007–1021.
2. Finch, R. G.; Pritchard, D. I.; Bycroft, B. W.; Williams, P.; Stewart, G. S. A. B. *J. Antimicrob. Chemother.* **1998**, *42*, 569–571.
3. Kjelleberg, S.; Molin, S. *Curr. Opin. Microbiol.* **2002**, *5*, 254–258.
4. Eberhard, A.; Burlingame, A. L.; Eberhard, C.; Kenyon, G. L.; Nealson, K. H.; Oppenheimer, N. J. *Biochemistry* **1981**, *120*, 2444–2449.
5. Kuo, A.; Blough, N. V.; Dunlap, P. V. *J. Bacteriol.* **1994**, *176*, 7558–7565.
6. Zhang, R. G.; Pappas, T.; Brace, J. L.; Miller, P. C.; Oulmassov, T.; Molyneaux, J. M.; Anderson, J. C.; Bashkin, J. K.; Winans, S. C.; Joachimiak, A. *Nature* **2002**, *417*, 971–974.
7. Vannini, A.; Volpari, C.; Gargioli, C.; Muraglia, E.; Cortese, R.; De Francesco, R.; Neddermann, P.; Marco, S. D. *Embo J.* **2002**, *21*, 4393–4401.
8. For a recent review, see Suga, H.; Smith, K. M. *Curr. Opin. Chem. Biol.* **2003**, *7*, 586–591.
9. Smith, K. M.; Bu, Y.; Suga, H. *Chem. Biol.* **2003**, *10*, 81–89.
10. Smith, K. M.; Bu, Y.; Suga, H. *Chem. Biol.* **2003**, *10*, 563–571.
11. Reverchon, S.; Chantegrel, B.; Deshayes, C.; Doutheau, A.; Cotte-Pattat, N. *Bioorg. Med. Chem. Lett.* **2002**, *12*, 1153–1157.
12. Givskov, M.; Nielsen, J. Int. Appl. WO Patent. 03,106,445, 2003; *Chem. Abstr.* **2004**, *140*, 42464u.
13. All new compounds gave ¹H NMR spectra in complete agreement with proposed structures.
14. Winson, M.; Swift, S.; Fish, L.; Throup, J.; Jorgensen, F.; Chhabra, S.; Siri, R.; Bycroft, B.; William, P.; Stewart, G. *FEMS Microbiol. Lett.* **1998**, *163*, 185–192.
15. Corpet, F. *Nucleic Acids Res.* **1988**, *16*, 10881–10890.
16. Thompson, J. D.; Higgins, D. G.; Gibson, T. J. *Nucleic Acids Res.* **1999**, *22*, 4673–4680.
17. Poirot, O.; Suhre, K.; Abergel, C.; O'Toole, E.; Notredame, C. *Nucleic Acids Res.* **2004**, *32*, W37–40.
18. Combet, C.; Jambon, M.; Deleage, G.; Geourjon, C. *Bioinformatics* **2002**, *18*, 213–214.
19. Schwede, T.; Kopp, J.; Guex, N.; Peitsch, M. C. *Nucleic Acids Res.* **2003**, *31*, 3381–3385.
20. Gouet, P.; Courcelle, E.; Stuart, D. I.; Metoz, F. *Bioinformatics* **1999**, *15*, 305–308.
21. Kabsch, W.; Sander, C. *Biopolymers* **1983**, *22*, 2577–2637.
22. Esnouf, R. M. *Acta Crystallogr. D* **1997**, *53*, 665–672.
23. SYBYL, Molecular Modeling System, Tripos Associates Inc., 1699 S. Hanley Road, St Louis, MO 63144-2913, USA.
24. Esnouf, R. M. *J. Mol. Graphics* **1997**, *15*, 132–134.
25. Birck, C.; Mourey, L.; Gouet, P.; Fabry, B.; Schumacher, J.; Rousseau, P.; Kahn, D.; Samama, J. P. *Structure* **1999**, *7*, 1505–1515.
26. Chai, Y.; Winans, S. C. *Mol. Microbiol.* **2004**, *51*, 765–776.
27. Krieger, E.; Koraimann, G.; Vriend, G. *Proteins* **2002**, *47*, 393–402.